Role of Step and Terrace Nucleation in Heteroepitaxial Growth Morphology: Growth Kinetics of CaF_2/Si(111)

Uwe Hessinger,* M. Leskovar, and Marjorie A. Olmstead

Department of Physics, University of Washington, Box 35-1560, Seattle, Washington 98195-1560

(Received 20 March 1995)

The thickness uniformity and the spatial distribution of lattice relaxation in thin (<8 nm) CaF_2/Si(111) films, observed with photoelectron spectroscopy and transmission electron microscopy, are seen to depend strongly on the initial nucleation kinetics. We develop a general model for heteroepitaxial growth that explains both these and literature results. Terrace or step nucleation leads to laminar films, although with different relaxation patterns; combined step and terrace nucleation leads to rough films due to different upper-layer nucleation rates on the differently sized islands.

PACS numbers: 68.55.Jk, 61.16.Bg, 68.55.Bd

Molecular beam epitaxial growth involves the deposition of atoms or molecules onto a crystalline surface. This is inherently a nonequilibrium process, and the evolving morphology of the growing film therefore depends on kinetics. The growth kinetics are controlled experimentally through the deposition flux and the substrate temperature, allowing access to a variety of growth regimes expressing different morphologies and epitaxial quality. In addition, intrinsic properties of the growing surface, including diffusion barriers and island or terrace sizes, influence the growth kinetics. These intrinsic properties evolve with growth for a heteroepitaxial system, increasing the complexity relative to homoepitaxy.

In this Letter, we propose a kinetic model to explain the variety of growth morphologies observed for the heteroepitaxial growth of CaF_2 on Si(111), and predict that similar behavior should be observed for other heteroepitaxial systems. We concentrate on CaF_2/Si films grown at temperatures above ~600 °C, for which the growth begins as a reacted Si-Ca-F layer that covers the surface completely [1,2]. The observed growth modes and morphologies for subsequent CaF_2 deposition vary from a fairly uniform morphology resulting from the coalescence of thin islands on the substrate terraces [Figs. 1(a) and 3(c)], through a nonuniform morphology characterized by thin islands on the substrate terraces and simultaneous thick islands along substrate step edges exhibiting multilayer (ML) growth [Figs. 1(b) and 3(a)], to solely step islands leading to layer-by-layer (LBL) growth after coalescence of ~5 layer thick step islands [Fig. 1(c)] [3] and via step flow [Fig. 1(d)] [4]. We propose that these different growth modes are due to different growth parameters, as indicated in Fig. 1.

The prediction of epitaxial growth kinetics involves the time scales for atomic deposition and diffusion. Myers-Beaghton and Vvedensky (MV) [5] introduced two dimensionless scaling parameters α and β to describe the kinetic regimes: $\alpha = Ja^2w^2/D$ is the ratio of the deposition rate per atomic site (flux J times the lattice constant squared, a^2) to the rate at which adatoms diffuse to a step edge (surface diffusion constant D divided by the terrace width squared, w^2); $\beta \approx w^2/a^2$ approximates the number of sites visited by an adatom as it diffuses to a step edge. For small α and β, adatoms will diffuse unimpeded to the step edge where they nucleate islands that grow along the step; for large α and β, the free adatoms are more likely to collide with each other before they reach the step, forming stable nuclei that grow into terrace islands. MV [5] distinguish three growth modes for homoepitaxial systems—step flow growth ($\alpha\beta < 1$), island formation ($\alpha > 1$), and a mixture of both ($\alpha < 1,\ \alpha\beta > 1$). For the heteroepitaxial case we discuss here, these modes correspond to step nucleation (SN), terrace nucleation (TN), and step and terrace nucleation (SN + TN), respectively.

Although the initial nucleation may be similar for homoepitaxy and heteroepitaxy, the resulting growth is different, since SN does not necessarily lead to step flow in heteroepitaxy. In homoepitaxy, step-nucleated "islands" form an extension of the terrace above the step; growth on top of them is thus identical to growth on the upper terrace.

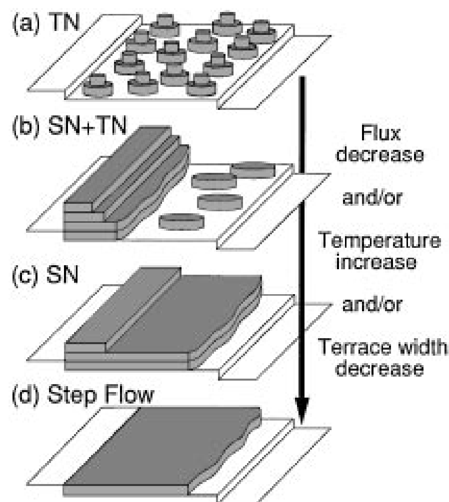

FIG. 1. Observed growth modes for CaF_2/Si(111) for different values of flux, substrate temperature, and terrace width. (a) Terrace nucleation (TN), (b) step and terrace nucleation (SN + TN), (c) step nucleation (SN), and (d) step flow. Note the nonuniformity in SN + TN due to the different heights of step and terrace islands.

 0031-9007/95/75(12)/2380(4)$06.00 © 1995 The American Physical Society

In heteroepitaxy, step islands are a different material than the substrate terrace, inducing a distinct growth mode.

In this paper we discuss the role of different first-layer nucleation modes in heteroepitaxial growth, in particular, first-layer step and terrace islands, on upper-layer nucleation and growth. These initial islands are reflected in the strain relaxation of the subsequent growth, observed with transmission electron microscopy (TEM) for CaF_2/Si(111). We find a nearly LBL growth for TN, and ML growth for SN + TN. Our general model, based on nucleation rate calculations, explains the data reported here, as well as observations by others that pure SN leads to LBL growth, either after coalescence at low coverage [3] or through step flow [4].

CaF_2 films were grown by molecular beam epitaxy on Si(111)–(7 × 7) substrates prepared by a chemical etch followed by annealing. The details are given in Ref. [6]. Films were characterized with x-ray photoemission spectroscopy and diffraction (XPS and XPD), and then capped by ~40 Å of amorphous Si for TEM. The plan view TEM images (taken on a Phillips 300 operating at 100 kV) show moiré fringes [7] indicative of regions where the CaF_2 has relaxed due to the ~2.6% lattice mismatch between CaF_2 and Si at the growth temperature (0.6% at room temperature). After cooling, the moiré fringe spacing indicates a final mismatch of ~1%, in agreement with other studies [7–10].

The morphologies of films for different initial nucleation regimes have been studied by combining TEM with XPS and XPD. In previous work [6,11], we used *in situ* XPS and XPD to obtain information on the average morphology of the first few molecular layers of CaF_2 deposited on Si as a function of substrate temperature and CaF_2 flux. These results are summarized as the open symbols in Fig. 2.

For growth parameters in region I (see Fig. 2) we observe a nonuniform average morphology. After about 35% of the interface layer is covered with a bilayer of CaF_2, upper layers begin to grow without significantly increasing the coverage of the Si-Ca-F layer. The interface layer is completely covered only after deposition of ~7 CaF_2 layers [6,11].

For growth parameters in region II we observe a more uniform average morphology. The initial bilayer covers about 75% of the interface layer before the next layer nucleates. Subsequent layers nucleate in an approximately layer-by-layer fashion, and uniform coverage of the Si-Ca-F layer is reached with only 3 CaF_2 layers [6,11].

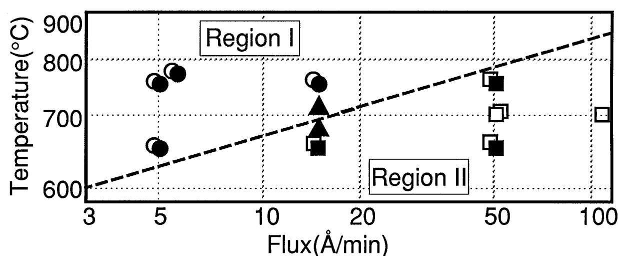

FIG. 2. Growth morphologies and nucleation regimes of CaF_2/Si(111) as a function of flux and substrate temperature. Nonuniform morphology (○), uniform morphology (□); step and terrace nucleation (●), terrace nucleation (■), transition regime (▲). Open symbols from XPS or XPD; closed symbols from TEM. Line separating regions I and II represents $\alpha = 1$.

In this paper, we relate the spatial distribution of islands, observed in TEM of somewhat thicker films (6–25 molecular layers), to the initial morphologies (closed symbols in Fig. 2). Bright field TEM images are shown in Fig. 3. In the growth regime characterized by nonuniform morphologies [region I, Fig. 3(a)], we observe relaxed regions (moiré fringes) along substrate steps that increase in size with increased film thickness. TEM showed about half the film to be relaxed at a nominal thickness of 80 Å (~25 layers). In the kinetic regime characterized by uniform coverage [region II, Fig. 3(c)], we observe relaxed regions distributed uniformly across the entire sample, with fractional coverage increasing with film thickness, but no indication of the initial step distribution. At intermediate flux and temperature conditions, a mixture of the two morphologies is observed [Fig. 3(b); denoted by triangles in Fig. 2].

We propose that the relaxed regions of the CaF_2 film reflect the initial nucleation. Relaxation of a strained film requires dislocations to nucleate and propagate. The relaxed regions therefore reflect regions where the activation barrier for this nucleation is reduced due to specific sites, such as step edges [12,13] of the substrate or of islands, or due to thickness beyond a critical thickness [14]. As shown in Fig. 3(c), the initial relaxation of the uniform-thickness films of growth parameter region II leaves white convex regions, which we associate with strained terrace islands, surrounded by relaxed regions. Upon coalescence, the relaxed edges of strained islands match up for sufficiently small islands but create defects for larger islands, which nucleate dislocations that cause relaxation between the islands [15]. The gliding of the dislocations into the middle of an island, and thereby relaxing it, is inhibited since the Burgers vectors of the $(a/2)\langle 110 \rangle$ type [9] do not lie in the interface, as reasoned by Tsai and Matyi [16]. The centers of strained islands eventually relax at increased coverage.

Uniform distribution of individual islands requires the initial nucleation of clusters across the entire terrace. For region II, the initial nucleation therefore is primarily TN, coalescing to a uniform morphology beyond 3–4 molecular layers [Fig. 1(a)].

In contrast, the nonuniform films of growth parameter region I show relaxed regions with high aspect ratios, parallel to each other and separated by about 1 μm [Fig. 3(a)]. These relaxed regions are thicker, step-nucleated islands along the substrate step edges. These islands nucleate upper layers at a smaller first-layer coverage than do terrace-nucleated islands, resulting in nonuniform films in the initial stages. Thin terrace islands are still present but have not relaxed. They can be observed for thicker films as strained regions framed by relaxed step islands that cover most of the surface, and in XPS or XPD by the coverage of the interface layer. The presence of terrace islands requires

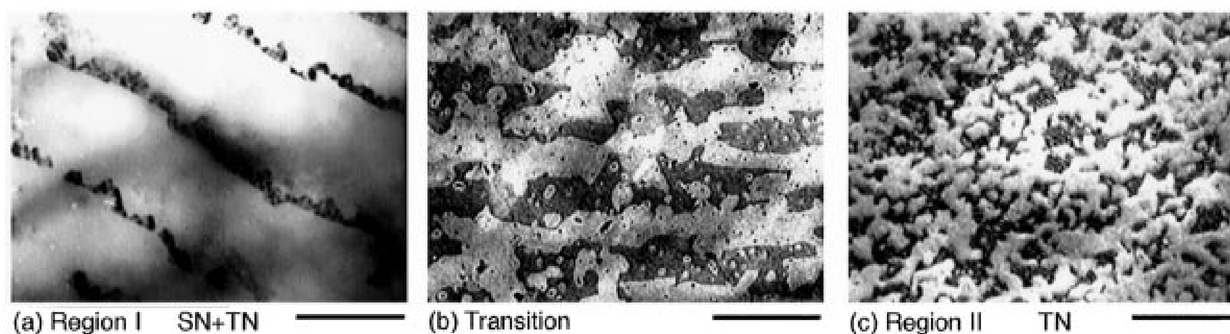

FIG. 3. Bright field TEM images of partly relaxed CaF_2/Si(111) films, with relaxed regions showing moiré fringes (darker regions). Note the relaxation along substrate steps separated by the terrace width of $w \sim 1$ μm in (a) and (b). Scale bars are 1 μm. Growth parameters (substrate temperature, flux, terrace width, thickness): (a) 775 °C, 5 Å/min, 1 μm, 40 Å; (b) 690 °C, 16 Å/min, 1 μm, 38 Å; and (c) 650 °C, 52 Å/min, 1 μm, 25 Å.

the existence of TN in addition to step-edge nucleation; we thus label region I as SN + TN [Fig. 1(b)].

In their discussion of homoepitaxial kinetics, MV [5] separate TN and SN + TN with $\alpha = Ja^2w^2/D = 1$, i.e., the time to deposit one monolayer equals the average diffusion time of an adatom to a step edge. The condition $\alpha = 1$ is fitted as a function of flux and temperature in Fig. 2, separating regions I and II. Assuming $D = a^2\nu \exp(-E_{d_1}/kT)$ with attempt frequency $\nu = 10^{13}$ s^{-1} ($\approx$ CaF_2 optical phonon frequency [17]), we deduce the diffusion barrier for CaF_2 molecules on the Si-Ca-F interface to be $E_{d_1} \approx 1.4$ eV.

The data for CaF_2/Si(111) can be summarized as follows. TN dominates in the kinetic regime $\alpha > 1$. It yields a uniform coverage beyond about three layers of CaF_2 on the reacted CaF interface, but the regions where islands coalesce form nucleation sites for subsequent relaxation. When CaF_2 molecules have a higher probability of reaching step edges ($\alpha < 1$, $\alpha\beta > 1$), nucleation occurs at both steps and terraces. The morphology of films with SN + TN is very nonuniform—at least in the initial stages—indicating that nucleation of additional layers is quite different on step- and terrace-nucleated islands.

We have never observed a single CaF_2 layer on top of the reacted Si-Ca-F layer in our investigated coverage range (>0.6 total CaF_2 deposited layers beyond the initial interface); rather we observe bilayers [6,11]. The covalently bonded interface Ca atoms are less ionized than in bulk CaF_2. This reduces the ionic attraction between the incident CaF_2 molecules and the Si-Ca-F effective substrate relative to that with subsequent CaF_2 layers, resulting in weaker binding energies and lower diffusion barriers on the interface layer than on subsequent layers [11]. Once CaF_2 molecules landing on the first CaF_2 layer nucleate a second layer, CaF_2 molecules diffusing on the weakly binding interface layer can gain energy by stepping up after the nucleation of the second layer until all upper sites are occupied and a bilayer is created. Similar behavior has been observed for CaF_2 on Si(111) for the nonreacted interface [18].

The difference in morphology for step- and terrace-nucleated islands we observe for CaF_2 on Si(111) should be a general feature of many heteroepitaxial systems. The principal material parameters used in our general model of the following paragraphs are the diffusion barriers of the substrate and of the deposited material, therefore encompassing different types of bonding, ionic or covalent, as well as different orientations of the surface. The model nevertheless is not strictly applicable to systems with strongly anisotropic surface diffusion, e.g., Si(100), which exhibits an effective one-dimensional surface diffusion along dimer rows.

When applying our general model to CaF_2/Si, the "substrate" (S) corresponds to the chemisorbed Si-Ca-F interface, the "first layer" ($L1$) corresponds to the *bilayer* of CaF_2, and the "second layer" ($L2$) corresponds to the actual *third* layer of CaF_2, and "atoms" or "adatoms" refer to CaF_2 molecules.

The critical issue for the relative lateral and vertical growth of islands is the $L1$ coverage at the time $L2$ nucleates. Atoms in $L2$, deposited on top of the $L1$ islands, can either diffuse across island edges and step down to $L1$ or, if the free adatom density is high enough on top of the island, form stable nuclei and initiate the growth of $L2$. If the coverage of $L1$ is complete when $L2$ nucleates, the growth evolves in a LBL fashion, whereas incomplete coverage results in a ML growth.

The critical size of an island, beyond which $L2$ nucleation occurs, has been calculated by Tersoff, Denier van der Gon, and Tromp [19] for the case of terrace islands in homoepitaxy. We extend these calculations to terrace and step islands in heteroepitaxy by considering the different sizes and shapes of these islands as well as the different diffusion constants D_1 and D_2 on S and $L1$, respectively. Round terrace islands are spaced apart by a nucleation distance [20] $\ell_n = (4a^2D_1/J)^{1/6}$. We assume that step islands extend a width L across the substrate terrace of width w. The SN calculation is done for an area of L^2, which contains the complete random walk of an adatom between deposition and reaching the island edge. The boundary conditions at the edges of the islands reflect the energetic barriers, often called Schwoebel barriers [21], which adatoms must overcome to cross step edges. From preliminary calculations, we find that island edges of CaF_2

exhibit negative Schwoebel barriers. The edge toward the upper terrace is assumed to reflect adatoms due to the step-induced defect [3] inherent in the twinned, type-B epitaxy [22]. Nevertheless, the results are qualitatively the same whether one or both edges act as sinks. For CaF_2 we assume a stable nucleus size of two molecules.

The critical size for $L2$ nucleation—width L_c for step islands and radius R_c for terrace islands—can be simplified by using the scaling parameters α and β, and expressed in terms of a critical coverage $\Theta_S = L_c/w$ for step islands and $\Theta_T = R_c^2/\ell_n^2$ for terrace islands,

$$\Theta_S \approx 1.8\left(\frac{a^2}{w^2}\frac{1}{\alpha\beta}\frac{D_2}{D_1}\right)^{1/7}, \quad \Theta_T \approx 1.5\left(\frac{D_2}{D_1}\right)^{1/4}. \quad (1)$$

For $D_2 < 0.2D_1$, as is the case for CaF_2 on Si(111), the terrace islands nucleate $L2$ at a coverage $\Theta_T < 1$. With a small diffusion coefficient in $L2$, it is harder for adatoms to diffuse to the island edge. This increases both the adatom density on top of the islands and the probability of nucleation of $L2$. The result for step islands includes $(a/w)^{2/7}$, which is a small number on the order of 0.1, and $(\alpha\beta)^{-1/7}$, which depends on the kinetic regime. For SN + TN, $\alpha\beta > 1$ and $\Theta_S < \Theta_T$; i.e., step islands in the kinetic regime of SN + TN nucleate upper layers at an earlier stage of growth than do terrace islands, resulting in a nonuniform morphology of thick step islands and thin terrace islands. By decreasing $\alpha\beta$, i.e., changing growth parameters towards a SN regime, Θ_S increases and step islands nucleate upper layers at a later stage of growth, eventually reaching step flow growth. The terrace width w has a strong effect on the growth mode, entering Θ_S as $(w^2\alpha\beta)^{1/7} \propto w^{6/7}$.

These calculations explain the observed morphologies for CaF_2/Si(111) shown in Fig. 1. The TN and SN + TN regimes are demonstrated in Figs. 2 and 3, which are described by $\alpha \approx 1$, $\alpha\beta \approx 10^7$. Substituting the experimental value $\Theta_T \approx 0.75$ at $T = 700$ °C implies $D_2/D_1 \approx 1/16$, or $E_{d_2} - E_{d_1} \approx 0.2$ eV. The two SN regimes in Fig. 1 are due to smaller terrace widths, as well as smaller fluxes, which decrease $w^2\alpha\beta$ and increase Θ_S, leading to no terrace islands and to more uniform morphologies. Coalescing SN islands were observed by Wong *et al.* [3] with experimental parameters ($J \approx 30$ Å/min, $w \approx 0.1$ μm) yielding $\alpha\beta \approx 60$. Tromp [4] has observed pure step flow, LBL growth, with growth parameters ($J \approx 0.6$ Å/min, $w \approx 0.1$ μm) yielding $\alpha\beta \approx 1$. Even though Eq. (1) does not yield $\Theta_S > 1$ for the latter case, the large difference in magnitudes for $\alpha\beta$ shows qualitative agreement with the heteroepitaxial theory. The morphologies change from fairly uniform to nonuniform, and back to uniform—a type of reentrant LBL behavior.

The physical reason that step islands lead to a nonuniform morphology for SN + TN, but to a more uniform morphology for SN, is that in the former case step islands are larger than terrace islands and therefore have *less* edge per area, and it is harder for adatoms in $L2$ to find the edge and leave. By changing growth parameters to reach pure SN, islands grow larger in $L1$ before nucleating $L2$. Since step islands are limited by the terrace width, there are always growth parameters for which step islands are too small to nucleate $L2$ before $L1$ is complete, leading to LBL growth.

We conclude that different experimental results for CaF_2/Si with the Si-Ca-F interface are due to different kinetic regimes of growth. For heteroepitaxy, step islands lead to second-layer nucleation at smaller (larger) first-layer coverage for SN + TN (SN) compared to TN. For growth of laminar films, the regime SN + TN should be avoided.

This work was supported by the Department of Energy under Contract No. DE-AC03-76SF00098 and Grant No. DE-FG06-94ER45516. We are grateful to J. D. Denlinger and E. Rotenberg for useful discussions.

*Electronic address: hessinger@u.washington.edu

[1] M. A. Olmstead, R. D. Bringans, R. I. G. Uhrberg, and R. Z. Bachrach, Phys. Rev. B **35**, 7526 (1987).
[2] D. Rieger, F. J. Himpsel, U. O. Karlsson, F. R. McFeely, J. F. Morar, and J. A. Yarmoff, Phys. Rev. B **34**, 7295 (1986).
[3] G. C. L. Wong, D. Loretto, E. Rotenberg, M. A. Olmstead, and C. A. Lucas, Phys. Rev. B **48**, 5716 (1993).
[4] R. M. Tromp (private communication).
[5] A. Myers-Beaghton and D. D. Vvedensky, Phys. Rev. B **42**, 5544 (1990).
[6] J. D. Denlinger, E. Rotenberg, U. Hessinger, M. Leskovar, and M. A. Olmstead, Phys. Rev. B **51**, 5352 (1995).
[7] D. Draheim, A. Tempel, A. Zehe, and D. Baither, Phys. Status Solidi A **119**, 209 (1990).
[8] K. G. Huang, J. Zegenhagen, J. M. Phillips, and J. R. Patel, Phys. Rev. Lett. **72**, 2430 (1994).
[9] H. Zogg, C. Maissen, S. Blunier, S. Teodoropol, R. M. Overney, T. Richmond, and H. Haefke, J. Cryst. Growth **127**, 668 (1993).
[10] S. Hashimoto, J.-L. Peng, W. M. Gibson, L. J. Schowalter, and R. W. Fathauer, Appl. Phys. Lett. **47**, 1071 (1985).
[11] J. D. Denlinger, E. Rotenberg, U. Hessinger, M. Leskovar, and M. A. Olmstead, Appl. Phys. Lett. **62**, 2057 (1993).
[12] S. Guha, A. Madhukar, and K. C. Rajkumar, Appl. Phys. Lett. **57**, 2110 (1990).
[13] Y. Fukuda, Y. Kohama, M. Seki, and Y. Ohmachi, Jpn. J. Appl. Phys. **28**, L19 (1989).
[14] J. H. van-der-Merwe, J. Electronic Mater. **20**, 793 (1991).
[15] S. V. Ghaisas and A. Madhukar, J. Vac. Sci. Technol. B **7**, 264 (1989).
[16] H. L. Tsai and R. J. Matyi, Appl. Phys. Lett. **55**, 265 (1989).
[17] A. Jockisch, U. Schröder, F. W. de Wette, and W. Kress, J. Phys. Condens. Matter **5**, 5401 (1993).
[18] R. M. Tromp and M. C. Reuter, Phys. Rev. Lett. **73**, 110 (1994).
[19] J. Tersoff, A. W. Denier van der Gon, and R. M. Tromp, Phys. Rev. Lett. **72**, 266 (1994).
[20] L. H. Tang, J. Phys. I (France) **3**, 935 (1993).
[21] R. L. Schwoebel and E. J. Shipsey, J. Appl. Phys. **37**, 3682 (1966).
[22] T. Asano and H. Ishiwara, Appl. Phys. Lett. **42**, 517 (1983).